fibers

MDPI

Article

Novel Bio-Functional Electrospun Membranes by Chios Mastic Gum Encapsulation

Panagiotis M. Mastorakis [1], Sotirios I. Marras [1,*], Costas Tsioptsias [2], Stephanos P. Zaoutsos [3], Demetres D. Leonidas [1], Ioannis Tsivintzelis [4,*] and Anna-Maria G. Psarra [1,*]

[1] Department of Biochemistry and Biotechnology, University of Thessaly, Biopolis, 41500 Larissa, Greece
[2] Department of Food Science and Technology, International Hellenic University, 57400 Thessaloniki, Greece
[3] Department of Energy Systems, University of Thessaly, Gaiopolis, 41500 Larissa, Greece
[4] Department of Chemical Engineering, Aristotle University of Thessaloniki, 54124 Thessaloniki, Greece
* Correspondence: smarras@bio.uth.gr (S.I.M.); tioannis@cheng.auth.gr (I.T.); ampsarra@uth.gr (A.-M.G.P.)

Abstract

Pistacia lentiscus var. *chia* resin (Chios Mastic Gum—CMG) is a natural aromatic resin that has been utilized in traditional medicine for more than 2.5 millennia, as it exhibits a wide range of pharmacological properties. In this study, various quantities of Chios Mastic Gum (3.5, 6.5, and 10 wt%) were encapsulated in electrospun fibers of poly-ε-caprolactone (PCL) to develop functional fibrous mats with multiple potential applications. The morphological analysis of composite membranes was conducted through scanning electron microscopy (SEM), revealing the formation of uniform fibers and incremental diameter size in samples with a higher concentration of CMG. The encapsulation efficiency was assessed by UV-Vis spectrophotometry and showed an exceptionally high loading efficiency (87–88%). The cytotoxicity of CMG-loaded nanofibers was tested in human embryonic kidney cell line HEK293 and human hepatocarcinoma cell line HepG2 using the MTT assay. In both cases, a high concentration of encapsulated CMG led to a statistically significant reduction in cell viability.

Keywords: Chios Mastic Gum; electrospinning; encapsulation; cytocompatibility; antitumor activity; polycaprolactone fibers

check for updates

Academic Editors: Lucian Lucia and Mazeyar Parvinzadeh Gashti

Received: 29 April 2025
Revised: 1 August 2025
Accepted: 21 August 2025
Published: 27 August 2025

Citation: Mastorakis, P.M.; Marras, S.I.; Tsioptsias, C.; Zaoutsos, S.P.; Leonidas, D.D.; Tsivintzelis, I.; Psarra, A.-M.G. Novel Bio-Functional Electrospun Membranes by Chios Mastic Gum Encapsulation. *Fibers* **2025**, *13*, 116. https://doi.org/10.3390/fib13090116

Copyright: © 2025 by the authors. Licensee MDPI, Basel, Switzerland. This article is an open access article distributed under the terms and conditions of the Creative Commons Attribution (CC BY) license (https://creativecommons.org/licenses/by/4.0/).

1. Introduction

Chios Mastic Gum (CMG) is a natural aromatic resin that is secreted by the shrub *Pistacia lentiscus* var. *Chia*, which is only found in the southern area of the Greek island of Chios. The resin itself has been recognized by the European Union as a Protected Designation of Origin (PDO) product [1], while the traditional process of its cultivation has been added to UNESCO's list of Intangible Cultural Heritage of Humanity [2]. Its unique properties have been utilized in a wide variety of fields, ranging from food, beverage, and pharmaceutical applications to industrial implementations in varnishes and adhesives.

CMG consists of more than 250 compounds [3], the combination of which provides its medicinal and aromatic properties. The first references of its benefits date back to the first century AD, when physician Dioscorides suggested its use against minor gastrointestinal disorders and for improving oral hygiene [4]. Since then, multiple studies have validated his observations and have shed more light on its positive effects on human health. Firstly, it has been used as a natural pharmaceutical compound for the eradication of H. pylori, a bacterium responsible for gastric ulcers [5]. Recent studies have demonstrated inhibition

of H. pylori strains in vitro [6,7], as well as its effectiveness against inflammatory bowel disease [8] and dyspepsia [9]. CMG, the first natural chewing gum, has been proven to be exceptionally beneficial for oral hygiene, protecting against gingivitis, the formation of plaque, xerostomia, and oral bacteria [10,11]. Its antimicrobial properties are also evident in foodborne pathogens and various common bacteria and fungi [12–14]. Moreover, it is rich in triterpenes, exhibiting anti-inflammatory activity via interference with glucocorticoid receptors (GRs), AMP-activated protein kinase (AMPK), peroxisome proliferator-activated receptor α (PPARα), and nuclear factor-kappa B (NF-κB) signaling [3,15,16]. When it comes to antioxidant effects, CMG has been proven to limit the production of H_2O_2 and superoxide via protein kinase C (PKC) inhibition [17], reduce the levels of oxidized low-density lipoprotein (oxLDL) [18,19], nitric oxide (NO), and prostaglandin E2 (PEG2), and scavenge hydroxyl radicals (•OH) [20], which is possible via the induction of antioxidant factors, such as PPARα expression [3]. Recent studies have also showcased its anti-proliferative and anti-metastatic properties in multiple cancer cell lines [21–24]. In addition, its consumption leads to improved prostate function [25], as well as lower cholesterol, triglyceride, and glucose levels [26,27]. Its most important recognition came in 2015, when the European Medicines Agency (EMA) classified CMG as a traditional herbal medicine and recognized its potency against dyspeptic disorders and skin inflammation as well as its ability to expedite the healing of small wounds [28].

However, in many cases, in vivo studies did not correspond with in vitro observations [29,30]. Many scientists have attributed these results to the sticky, non-soluble polymer, which constitutes 25–30% of CMG. The polymer is considered responsible for interfering with bioactive compounds, for increasing difficulty in sample handling, and for reducing water solubility and bioavailability [6]. As a result, most recent investigations have focused on the total mastic extract without polymer (TMEWP). Nevertheless, in some studies, the removal of the polymer led to a reduction in CMG's activity [27,31].

Recently, there has been a significant surge in interest in developing innovative products to utilize and enhance CMG's activity. These studies aim to encapsulate CMG in silver [32,33] or polymer-based nanoparticles [34] and nanostructured lipid carriers [14,35,36], mainly for cutaneous applications.

Another method that can elevate its properties is electrospinning, which is a fast, simple, and economic technique that is based on using electrostatic forces to produce porous membranes consisting of ultrathin polymeric fibers. These fibers, whose average diameter ranges from a few nanometers to micrometers, can be functionalized by incorporating bioactive substances, which can enhance their performance for various biomedical applications, such as drug delivery [37], cancer treatment [38], or wound healing [39]. Functionalized membranes are capable of providing sustained and targeted release, enhancing their effectiveness and limiting the possibility of side effects due to drug overdoses or direct contact with the skin with some pure extracts in topical treatments. Their interconnected porous network allows water vapor and oxygen molecules to diffuse efficiently through the fibrous membrane, maintaining an appropriate moisture level in the area around the wound and promoting tissue regeneration [40]. Moreover, fibrous mats exhibit excellent biocompatibility, and their composition allows them to mimic the native extracellular matrix (ECM), expediting cell proliferation and wound healing [41]. These membranes have increased mechanical strength, and they are thin and lightweight with high flexibility, which allows them to adapt to various surfaces, such as the skin's contours or tissues [39]. Evidently, the encapsulation of CMG in electrospun fibers could result in a novel product with enhanced bioactive properties.

For the fabrication of effective electrospun membranes, the selection of a polymer with suitable properties is crucial. Especially for the development of medical devices, their

toxicity, immunogenicity, and ability to encapsulate active pharmaceutical ingredients should be taken into consideration. In this regard, poly-ε-caprolactone (PCL) is a promising choice for the encapsulation of CMG, as it is a biocompatible and biodegradable polymer, exhibiting exceptional blend compatibility, low solubility, and slow degradation [42].

Thus, this study focused on the development of CMG-functionalized PCL fibrous mats and on the analysis of the physicochemical and biological characteristics of the composite membranes. Initially, membrane samples containing various quantities of CMG (3.5, 6.5, and 10 wt%) were prepared by electrospinning. Since it is the first time that CMG was encapsulated into electrospun fiber mats, a relatively low concentration of CMG was selected for initial experiments (i.e., 3.5 wt%) and was increased approximately 3 times (up to 10 wt%). An investigation into the morphology of the fibers was carried out through scanning electron microscopy (SEM), and the encapsulation efficiency was determined through UV-Vis spectrophotometry. Studies of the thermal behavior of the produced mats included thermogravimetric analysis (TGA) and differential scanning calorimetry (DSC). The cytocompatibility of the electrospun fibers, as well as their anticancer activity, was examined via an MTT assay by measuring the viability of HEK293 and HepG2 cells, respectively. To the best of our knowledge, this is the first time that CMG is encapsulated into electrospun polymer membranes, which will probably broaden the application field of the bioactive substance.

2. Materials and Methods

2.1. Materials

The Chios Mastic Gum (CMG) powder was a kind donation from the Chios Mastic Growers Association and mastihashop. Poly-ε-caprolactone (PCL), dichloromethane (DCM), and dimethylformamide (DMF) were obtained from Sigma-Aldrich (St. Louis, MO, USA), while Dulbecco's modified Eagle medium (DMEM) (with 4.5 g/L glucose and 1 mM sodium pyruvate), trypsin–EDTA 1X in PBS, L-glutamine, penicillin–streptomycin solution 100X, fetal bovine serum (FBS), and MTT (3-(4,5-dimethylthiazol-2-yl)-2,5-diphenyltetrazolium bromide) were purchased from Biowest (Nuaillé, France). In this study, 2-hydroxy-5-methylbenzaldeyhyde (BLD Pharmatech, Shanghai, China), ethanol, dimethyl sulfonyl chloride (DMSO) (AppliChem GmbH, Darmstadt, Germany), and sulfuric acid (Scharlau, Barcelona, Spain) were also used. The two cell lines (HEK293 and HepG2) involved in this study were purchased from the American Type Culture Collection (ATCC) (Wesel, Germany).

2.2. Electrospinning

Initially, PCL was dissolved at a concentration of 11.5% (*w*/*v*) in a solvent mixture of DCM and DMF at a 3:1 volume ratio [43,44]. Various concentrations of CMG were added to the solution to form composite membranes. Solutions were incubated overnight at room temperature to ensure a fully homogeneous state.

Electrospinning was performed with a homemade apparatus. The solutions were inserted into a glass syringe (5 mL internal volume, 20 G, 0.603 needle internal diameter), and the flow rate was controlled by a syringe pump (Harvard Apparatus, model 2274, Holliston, MA, USA). The syringe tip was connected to a high voltage power supply (Spellman High Voltage DC Supply, model RHR30P30, New York, NY, USA), and the produced fibers were deposited on a rotating drum (10 rpm) covered with aluminum foil.

All the experiments were carried out at room temperature and humidity. The flow rate was constantly set to 0.5 mL/h, the applied voltage was equal to 15 kV, and the syringe tip was positioned at a distance of 7 cm from the collector [43,44]. The resulting membranes were inserted in a vacuum chamber overnight (Shanghai Laboratory Instrument

Works Co. Ltd., model 320 Pa, Shanghai, China) for the evaporation of moisture and residues of DCM and DMF. Hence, composite mats containing 0, 3.5, 6.5, and 10 wt% CMG were produced, which were named "Pure PCL", "PCL/3.5CMG", "PCL/6.5CMG", and "PCL/10CMG", respectively.

2.3. Physicochemical Characterization of the Electrospun Mats

2.3.1. Morphological Characterization

In order to obtain information about the morphology of the produced fibers, the samples were observed through a scanning electron microscope (JSM-6510, Jeol, Tokyo, Japan; operated at an accelerating voltage of 20 kV). Carbon coating of the samples was conducted through a rotary pumped coater (Quorum, model Q150R ES, Sussex, England) to prevent charging. Secondary electron images were obtained under high-vacuum conditions, with a working distance of 10 mm and at various magnifications (ranging from ×350 to ×2000). Using the acquired SEM images, the fibers' diameters for each sample were determined by analyzing 100–150 fibers from at least two different areas of the sample, in order to ensure representative sampling, using ImageJ software (version 1.54) [45]. The measurement was performed manually using the straight-line tool, and the scale was set based on the scale bar of the SEM images.

2.3.2. Encapsulation Efficiency and Drug Loading

The quantification of the CMG on the surface and inside the fibrous mats was determined by a UV-Vis method for the detection of triterpenes [46]. The methodology was adapted to CMG, which consists of 65–70% triterpenes [8]. For each measurement, 3 mg of a composite membrane was dissolved in DCM, and an appropriate volume of the solution was transferred into a new container, so that the theoretical amount of CMG was equal to 0.1 mg. After evaporation of the solvent, 1 mL of an ethanol solution of 1% 2-hydroxy-5-methylbenzaldeyhyde and 0.75 mL of sulfuric acid were added. After 25 min of incubation at room temperature, the samples were placed in ice for 5 min to stop the reaction. Then, the absorption of the samples was measured at 543 nm using a UV-Vis spectrophotometer (VWR International, model 1600-PC, Radnor, PA, USA) with a 1 cm path-length quartz cuvette. In each case, the blank sample contained the appropriate theoretical amount of PCL without CMG. A standard curve of pure CMG was prepared and utilized for quantification purposes. Finally, the entrapment efficiency and the true wt% of CMG in the fibers were calculated based on Equations (1) and (2), respectively.

$$\text{Encapsulation Efficiency } (\%) = \frac{\text{Actual amount of CMG}}{\text{Theoretical amount of CMG}} \times 100 \quad (1)$$

$$\text{Drug loading } (\%) = \frac{\text{Actual amount of CMG}}{\text{Total mass of sample}} \times 100 \quad (2)$$

2.3.3. Analysis of Thermal Behavior

The thermal characteristics of the composite membranes were investigated by thermogravimetric analysis (TGA) and differential scanning calorimetry (DSC). In TGA, approximately 3–5 mg of each sample was placed in a thermogravimetric analyzer (Shimadzu Instrument Ltd., model TGA-50, Kyoto, Japan) and was heated from room temperature to 600 °C to assess thermal stability and degradation behavior. TGA measurements were performed using a heating rate of 10 °C min^{-1} under a constant nitrogen flow of 20 cm^3 min^{-1}.

Regarding DSC, a differential scanning calorimeter was used (Shimadzu Instrument Ltd., model DSC-50, Kyoto, Japan), and the temperature ranged from 45 °C to 200 °C to determine thermal transitions. DSC measurements were performed using a heating rate of

10 °C min^{-1} under a constant nitrogen flow of 20 cm^3 min^{-1}. Prior to heating, 3–5 mg of each sample was placed in a metallic pan, which was properly sealed. An empty sealed metallic pan was used as a reference.

2.4. Biological Characterization of the Electrospun Mats

2.4.1. Cell Culture and Seeding

HEK293 (human embryonic kidney-derived cells) and HepG2 (human liver cancer cells) cell lines, widely applied for the biological assessment of natural products [47,48], were involved in our study. In both cases, the cells were cultivated in suitable 25 or 75 cm^2 culture flasks, which contained DMEM (with 4.5 g/L glucose and 1 mM sodium pyruvate) supplemented with 10% FBS, 2 mM L-glutamine, and 1% penicillin–streptomycin solution (100×). The cells were grown in an incubator (New Brunswick Scientific, model Galaxy 170S, San Diego, CA, USA) at 37 °C in 5% CO_2. Cells were passaged every 3–4 days when the confluence of the flask reached approximately 90%. During cell seeding, a hemocytometer (Heinz Herenz Medizinalbedarf GmbH, Hamburg, Germany) was used to count the cells that were seeded in a 96-well plate containing 200 μL of a cell culture medium per well. All cell culture experiments were conducted under sterile conditions in a laminar flow hood (Telstar, model av-30/70, Barcelona, Spain).

2.4.2. Cell Viability/MTT Assay

The cytotoxic effect of CMG-functionalized PCL fibrous mats was assessed on HEK293 and HepG2 cell lines. A total of 5000 and 8000 cells, respectively, were seeded in 96-well plates and incubated for 24 h. Samples of composite membranes were added to the wells, and their effect after 48 h was assessed through the MTT assay. Before their addition, samples were prepared by creating circular disks (with diameters equal to 4 mm) using a hole punch set (Paffrath, model 0800320, Le Thieulin, France), and each sample side was UV-sterilized for 30 min under the laminar flow hood.

The MTT assay enables colorimetric detection of metabolically active cells. This method is based on the reduction of the MTT reagent to insoluble formazan by mitochondrial succinate dehydrogenase of living cells, leading to the formation of formazan crystals. Solubilization of formazan crystals leads to the development of a purple color. Initially, cells were incubated for 3–4 h in a cell culture medium containing 0.5 mg/mL MTT reagent. Then, the medium was carefully removed, 150 mL of DMSO was added, and the plate was positioned on a shaker (Gesellschaft für Labortechnik, model 3015, Burgwedel, Germany) and subjected to gentle agitation until the crystals were fully dissolved. Subsequently, 100 mL from each well was transferred to a new 96-well plate to avoid interference from the circular membrane samples. The absorbance at 570 and 690 nm (background) was measured using a plate reader (Perkin Elmer, model Enspire2300, Waltham, MA, USA). The final absorbance of each well was calculated by subtracting the absorbance value of the background from the absorbance value at 570 nm. Cell viability was calculated using Equation (3).

$$\text{Cell Viability } (\%) = \frac{\text{Average final absorbance of treated cells}}{\text{Average final absorbance of untreated cells}} \times 100 \quad (3)$$

For each concentration of CMG, at least 3 samples were analyzed, and statistical significance was assessed using Welch's *t*-test.

3. Results and Discussion

3.1. Physicochemical Properties of the Electrospun Mats

3.1.1. Morphological Characteristics

Scanning electron microscopy (SEM) was utilized to analyze the morphology of poly-ε-caprolactone (PCL) fibers with various amounts of encapsulated Chios Mastic Gum (CMG) (0, 3.5, 6.5, and 10 wt%). A visual representation of the fibers is depicted in Figure 1. The electrospun fibers exhibited a homogeneous morphology without beads, especially in samples with a lower concentration of CMG.

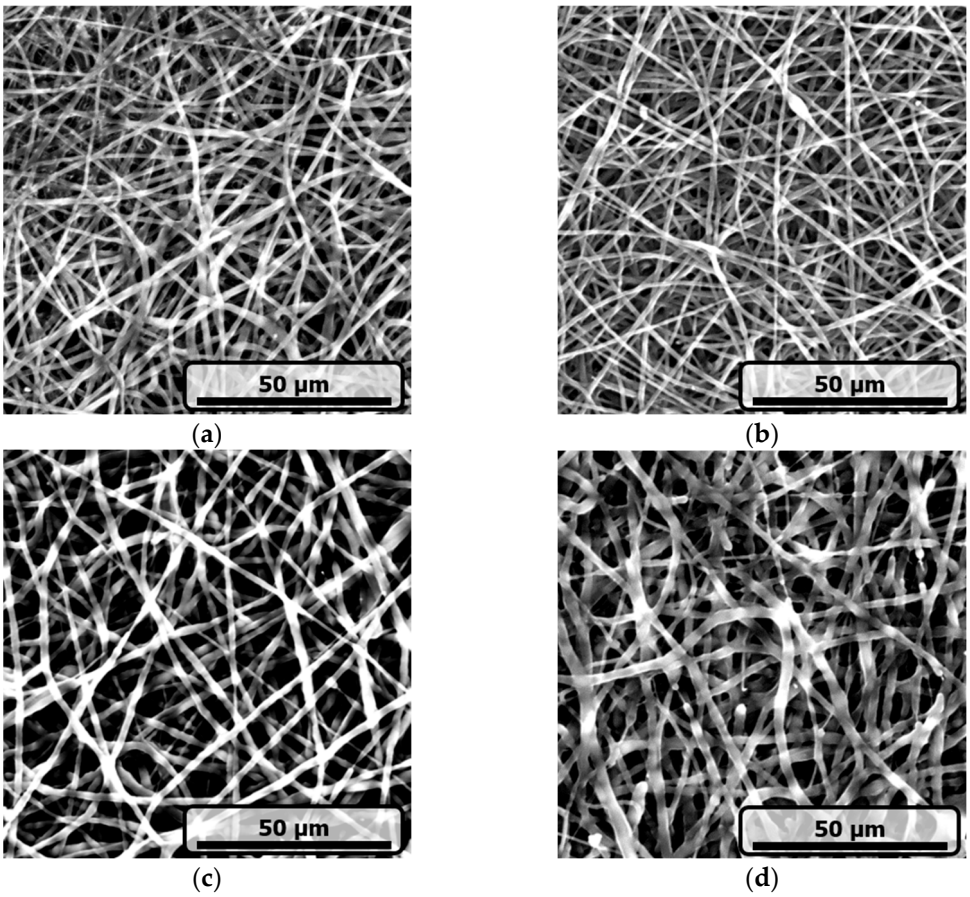


Figure 1. SEM images depicting the morphology of electrospun fibers of (**a**) neat PCL, (**b**) PCL/3.5CMG, (**c**) PCL/6.5CMG, and (**d**) PCL/10CMG samples.

The average diameter of the fibers, which is presented in Figure 2, ranged from approximately 1.25 to 1.9 μm. An increase in CMG concentration led to a small increase in the average fiber diameter. This result can be attributed to the increased viscosity of the solution caused by the rise in CMG content. This increase is due to the composition of CMG, which contains the natural polymer *cis*-1,4-poly-β-myrcene, as mentioned in the Introduction Section. Thus, dissolution of CMG elevates the solution's viscosity, owing to the natural polymer's presence, and leads to the formation of thicker fibers. Solution viscosity is a crucial factor that significantly influences the quality of the prepared fibers. Various studies have highlighted that an increase in this parameter impedes the solution's flow, and the electrospinning jet becomes less fluid and more difficult to stretch, resulting in the production of fibers with larger diameters [49–51].

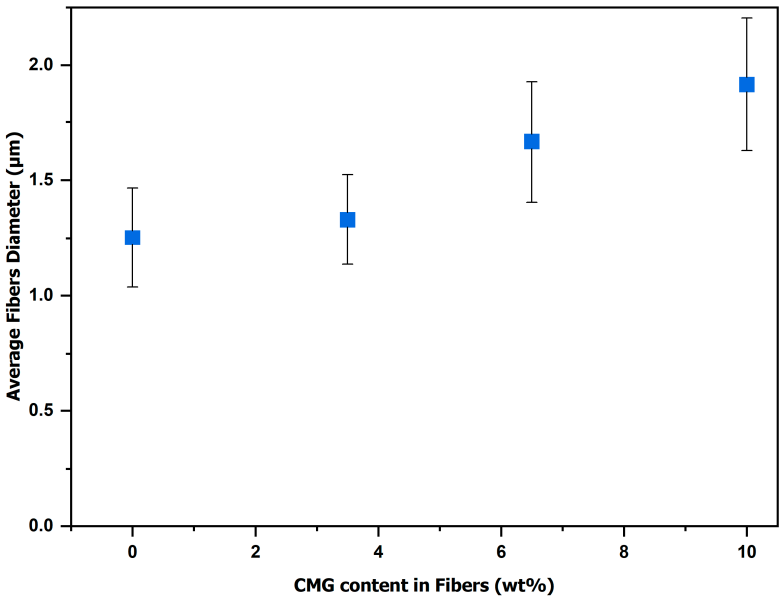


Figure 2. Effect of increasing the concentration of CMG on the average diameter of electrospun PCL fibers. Data are depicted as average value ± standard deviation (n = 100–150).

3.1.2. Encapsulation Efficiency and Drug Loading

The actual amount of CMG compared to its theoretical value, as well as the true wt% in the fibers, was determined through a UV-Vis method and is displayed in Table 1. In all samples, the entrapment efficiency was exceptionally high, reaching 87–88%.

Table 1. Encapsulation efficiency (%) and CMG loading (wt%) of composite mats. Data are depicted as average value ± standard deviation (n = 2–4).

Samples	Encapsulation Efficiency (%)	CMG Loading (wt%)
PCL/3.5CMG	87 ± 6	3.0 ± 0.2
PCL/6.5CMG	88 ± 3	5.7 ± 0.2
PCL/10CMG	87 ± 5	8.7 ± 0.4

The encapsulation efficiency depends on various parameters such as the processing variables [52], the selection of an appropriate solvent, and the intermolecular interactions between the drug and the polymer [53]. A proper selection of a drug–polymer–solvent system can enhance drug solubility and stabilize the drug within fibers. Consequently, it significantly improves drug loading efficiency and affects the kinetics of the drug release [54,55]. Another important factor is drug concentration, which may also affect loading efficiency. Böncü & Özdemir [56] noticed that at low drug content, the encapsulation efficiency is very high, but beyond a certain value, it drops due to the undissolved drug in the solution. On the contrary, other studies showed a successful encapsulation of very high drug loadings (up to 60%) [57,58]. Hence, the drug content is an important factor affecting the encapsulation efficiency, but it is not the only one, since the latter (encapsulation efficiency) depends on multiple processing parameters and the synergistic effects between the compounds of the ternary system (drug–polymer–solvent).

3.1.3. Thermal Behavior

Thermal analysis of the neat and composite fibers was performed by thermogravimetric analysis (TGA) and differential scanning calorimetry (DSC). TGA thermograms are presented in Figure 3. High similarity is exhibited among all samples, with the maximum decomposition rate ranging from 402 to 409 °C. Samples with higher CMG content exhibit

a small shift in decomposition initiation to lower temperatures, as well as prolonged degradation at higher temperatures. This trend can be explained by the TGA behavior of pure CMG, presented in a recent study [59], in which CMG's degradation starts at ≈227 °C and is completed at ≈490 °C. Hence, an increase in CMG leads to profiles with a higher resemblance to that of pure CMG.

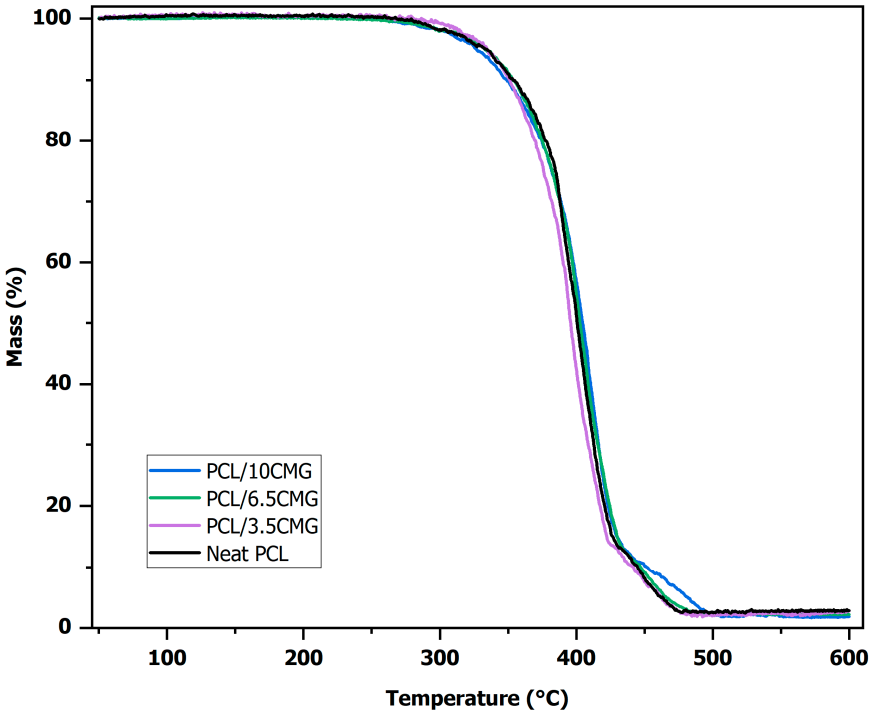


Figure 3. TGA thermograms of neat PCL, PCL/3.5CMG, PCL/6.5CMG, and PCL/10CMG samples in nitrogen atmosphere.

The latter is better understood when keeping the encapsulation mechanism in mind. During electrospinning, solvent evaporation occurs rapidly and induces the rapid solidification of the polymer and the drug. In most cases, solidification proceeds independently, and a two-phase (solid–solid) mixture is formed. However, this mechanism is expected to be more complicated in the case of CMG, since it is not a single drug substance, but a multicomponent mixture of various compounds. Nevertheless, as mentioned above, CMG is mainly composed of triterpenes, which are hydrocarbons and, as such, are of low polarity. On the contrary, PCL presents moderate polarity due to the presence of the polar C=O and C-O groups. Thus, a strong compatibility between PCL and CMG is not expected. Due to the higher content of PCL, the polymer acts as the continuous matrix, and micro- and nano-phases (particles) of CMG are expected to be present inside the matrix and on the surface of the fibers. This behavior suggests the absence of strong interactions between the polymer and the drug, and thus, no alteration of the biochemical properties and bioactivity of the drug is expected. Consequently, PCL nanofibers can be considered as inert and safe carriers for CMG.

DSC graphical data are depicted in Figure 4. Initially, the first heating scan was evaluated in order to account for the effect of the rapid solidification/crystallization of the matrix due to the rapid evaporation of the solvent during electrospinning and the effect of the high surface-to-volume ratio that nano- or micro-fibers exhibit. It is known that PCL exhibits a sub-zero glass transition temperature and a sub-zero crystallization temperature. However, the materials developed in this study are meant for biomedical applications and, thus, any shifting of the sub-zero transitions is of low practical importance. Consequently,

the DSC measurements were performed starting from 45 °C. In addition, no thermal effect is expected for PCL at temperatures above its melting point, which is around 60 °C. However, CMG is a mixture of various substances, and some thermal effects, e.g., evaporation, may occur. For this reason, the DSC measurements were performed up to 200 °C, which is a temperature close to the temperature of the decomposition initiation of CMG. As presented in Figure 4, in all cases, an endothermic peak around 60 °C is present, which corresponds to the melting of PCL. A slight shift in the peak to lower temperatures is observed, as the quantity of CMG increases, i.e., a melting point of 60.8 °C is observed for neat PCL fibers, which reduces to 60.1 °C, 58.3 °C, and 58.3 °C upon the addition of 3.5, 6.5, and 10%wt CMG, respectively.

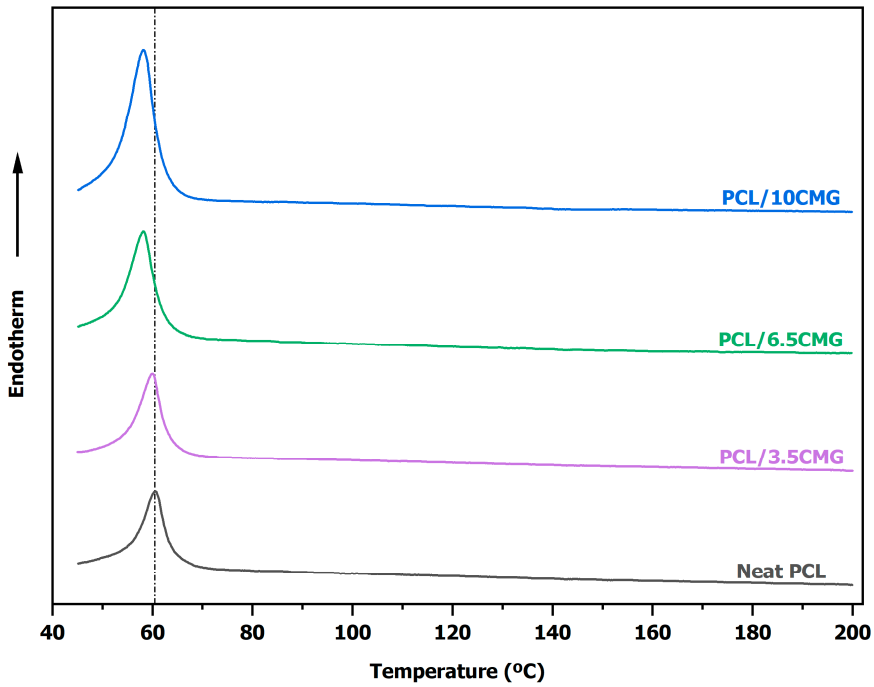


Figure 4. DSC heating thermograms of neat PCL, PCL/3.5CMG, PCL/6.5CMG, and PCL/10CMG samples in nitrogen atmosphere.

Next, two subsequent DSC scans were performed. Initially, samples were heated up to 100 °C in order to completely melt (first scan); then, they were cooled down to 30 °C (for approximately 30 min) and subsequently heated (second scan) again up to 100 °C. The results are presented in Figures 5 and 6. In Figure 5, the melting point of both scans is presented, while in Figure 6, the crystallinity of the samples is presented. The results reveal that the untreated samples, as produced by electrospinning, present a higher melting point and higher crystallinity. In all cases, similarly to the results presented in Figure 4, the melting point is marginally reduced as the CMG content increases. Furthermore, as presented in Figure 6, the crystallinity shows a maximum for CMG content around 6%wt.

The small reduction in the melting point with the CMG content is a usual behavior in composite polymer materials and is attributed to the easier destruction of the semicrystalline polymer structure due to the addition of the inert compound, i.e., the additive hinders the development of large crystallites and, in many cases, acts as a nucleating agent that promotes heterogeneous nucleation, which also results in more, but smaller, polymer chain crystallites that are destroyed at lower temperatures [43,44]. A similar response of drug-loaded electrospun fibers was reported in previous studies [43,44].

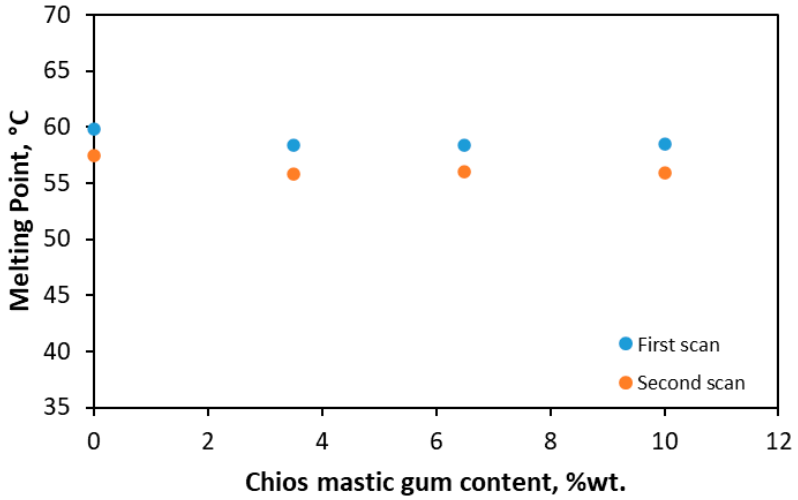


Figure 5. Melting point of neat PCL, PCL/3.5CMG, PCL/6.5CMG, and PCL/10CMG samples as measured by DSC in two subsequent scans.

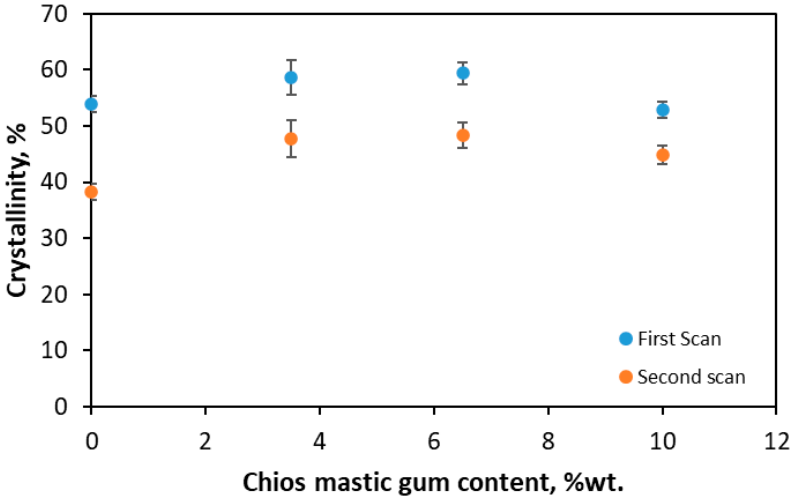


Figure 6. Crystallinity of neat PCL, PCL/3.5CMG, PCL/6.5CMG, and PCL/10CMG samples as measured by DSC in two subsequent scans.

The addition of the inert compound has a double effect on the crystallinity of the composites. Firstly, it induces heterogeneous nucleation, which tends to increase crystallinity, but at the same time, it tends to reduce the overall crystallinity of the composite material, since it is not crystalline itself and hinders the growth of large polymer crystallites. The occurrence of such two competitive effects results in a maximum for crystallinity, as presented for both scans in Figure 6, as well as Figure S1 and Table S1 of the Supplementary Material file.

3.2. Biological Proberties of the Electrospun Mats

3.2.1. Determination of Cell Viability on HEK293 Cells

The effect of CMG-loaded fibers on the cell viability of human embryonic non-cancerous HEK293 cells was evaluated by an MTT assay after incubation for 48 h. The results are depicted in Figure 7. The sample containing the highest concentration of CMG (PCL/10CMG) exhibited statistically significant cytotoxicity, resulting in a 20% reduction in cell viability. A lower concentration of encapsulated CMG did not cause statistically significant cytotoxicity in accordance with previous observations, revealing a cut-off of approximately 40 μg/mL–60 mg/mL of different polarity CMG fractions to induce cytotoxic

effects [15]. Thus, cytotoxic effects of CMG fractions have been observed in a previous study, in which concentrations as high as 60 μg/mL exhibited a statistically significant inhibition of cell proliferation, varying from 20% for apolar and polar fractions to 50% for medium-polar fraction [15]. Examination of apoptotic and anti-apoptotic protein levels by Western blot analysis showcased a significant decrease in procaspase-3, procaspase-9, and bcl-2, indicating the role of CMG in apoptosis induction by the mitochondrial intrinsic pathway. Both the anti-inflammatory and regulatory role of CMG fractions on cellular energy metabolism is exhibited [15]. The outcome of analogous experiments of HEK293 cell viability was similar for fractions from CMG leaves [60], but not for mastic oil, which did not exhibit statistically significant cytotoxicity at the highest concentration tested (85 mg/mL) [21]. These results indicate that focused research, depending on the desired application, should be conducted (e.g., effect on dermal fibroblasts for cutaneous applications).

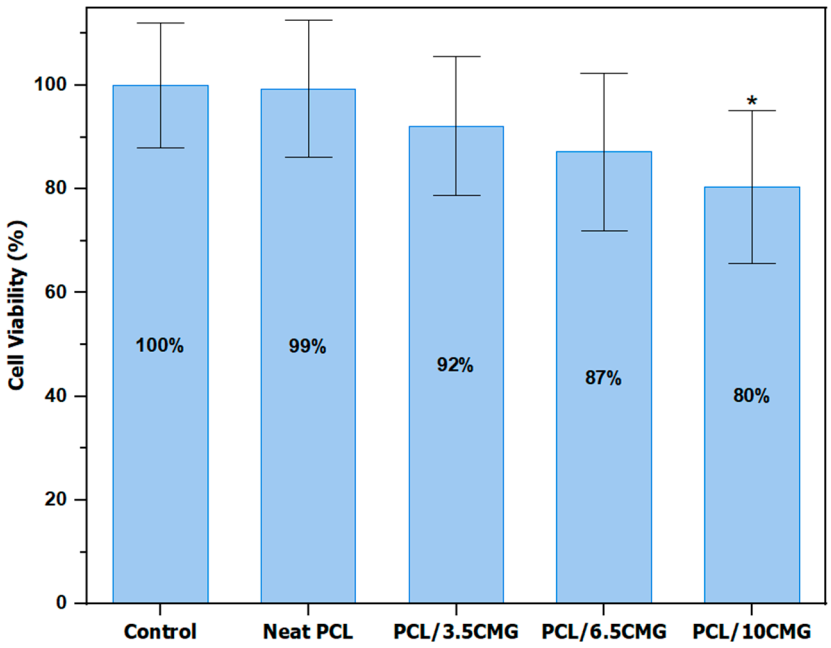


Figure 7. Effect of neat PCL, PCL/3.5CMG, PCL/6.5CMG, and PCL/10CMG samples on HEK293 cell viability. Data are depicted as average value ± standard deviation (n = 4–6; * $p < 0.05$ compared to control).

3.2.2. Determination of Cell Viability on HepG2 Cancer Cells

CMG is well known for its potential gastrointestinal therapeutic effects [4]. Thus, the in vitro antitumor activity of CMG-functionalized PCL fibrous mats was assessed on human hepatocarcinoma HepG2 cells via the MTT assay. The results were similar to those on HEK293 cells and are presented in Figure 8. The composite membranes with the highest concentration of CMG (PCL/10CMG) resulted in a statistically significant reduction in cell viability equal to 28%. The enhanced anti-proliferative activity of CMG-functionalized PCL fibrous mats in carcinoma cells compared to that in the immortalized non-cancerous HEK293 cells could possibly indicate potential beneficial cytotoxic activities of the CMG-functionalized PCL fibrous mats against cancer cells. These observations correspond to findings of a recent study [14], in which fractions of CMG entrapped in liposomes led to significant limitations in HepG2 cell growth. Another study demonstrated the cytotoxic effect of both total mastic extract with and without the polymer at concentrations of 100 μg/mL [61]. Furthermore, CMG anticancer properties have also been observed in colorectal (HCT116) [24], prostate (PC-3 and LNCaP) [62,63], leukemia (HL-60) [64], breast (MCF-7) [14], pancreatic (COLO 357 and BxPC-3) [65], and oral (YD-10B and SCC25) [66,67]

cancer cells. Furthermore, the unique properties that PCL displays render it a powerful tool that has been widely used in many biomedical applications, including anticancer drug delivery systems [68–70].

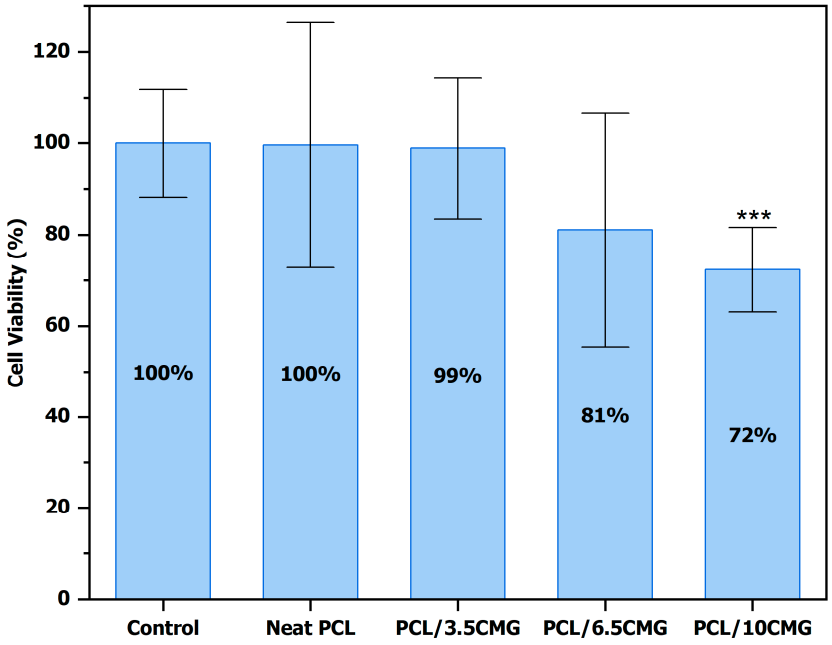


Figure 8. Effect of neat PCL, PCL/3.5CMG, PCL/6.5CMG, and PCL/10CMG samples on HepG2 cell viability. Data are depicted as average value ± standard deviation (n = 3–6; *** $p < 0.001$ compared to control).

4. Conclusions

In this study, encapsulation of various concentrations of Chios Mastic Gum (0, 3.5, 6.5, and 10 wt%) in PCL fibers by electrospinning was achieved for the first time. CMG is a traditional herbal medicine with multiple biological activities, while electrospinning enables the sustained release of encapsulated drugs and increased bioavailability. This combination could lead to the production of innovative and promising composite membranes, which could potentially be used in pharmaceutical, cosmetic, and biomedical applications.

The fabricated electrospun membranes exhibited high homogeneity and the absence of beads. Furthermore, an increase in CMG loading resulted in a small increase in fiber diameter, while encapsulation of CMG was remarkably efficient, reaching 87–88%. Evaluation of their cytotoxicity on HEK293 and HepG2 cells via the MTT assay demonstrated a statistically significant decrease in cell viability upon a 48 h incubation of the cells with the samples with the highest CMG content (10 wt%). Furthermore, 10 wt% CMG-functionalized PCL fibrous mats also exhibit slightly enhanced cytotoxic effects against carcinoma cells, indicating potential future applications for cancer treatment. No significant cytotoxicity was observed in samples with lower concentrations of CMG.

Further investigations of CMG-functionalized PCL fibrous membranes could showcase further medicinal potential in terms of antimicrobial and anti-inflammatory properties, which have been established in the existing literature for pure CMG, highlighting its potential application in wound healing and dermal disorders such as acne and cancer. An evaluation of the in vitro release of CMG is also a crucial step for a deeper understanding of the activity of composite membranes.

Supplementary Materials: The following supporting information can be downloaded at https://www.mdpi.com/article/10.3390/fib13090116/s1: Figure S1. Thermograms of the first (**a**) and second DSC scans (**b**), with data referring to the results of Table S1 and Figures 5 and 6 of the main article; Table S1. DSC results referring to Figures 5 and 6 of the main article.

Author Contributions: Conceptualization, S.I.M., I.T. and A.-M.G.P.; methodology, P.M.M.; D.D.L., C.T., S.P.Z., I.T., S.I.M. and A.-M.G.P.; validation, P.M.M., C.T., I.T., A.-M.G.P. and S.I.M.; investigation, P.M.M., D.D.L., C.T., S.P.Z., I.T., S.I.M. and A.-M.G.P.; resources, I.T., S.I.M. and A.-M.G.P.; writing—original draft preparation, P.M.M.; writing—review and editing, I.T., A.-M.G.P. and S.I.M.; visualization, P.M.M. and S.I.M.; supervision, I.T., A.-M.G.P. and S.I.M.; funding acquisition, A.-M.G.P. and S.I.M. All authors have read and agreed to the published version of the manuscript.

Funding: This research was partially supported by the Postgraduate Program "Application of Molecular Biology-Genetics-Diagnostic Biomarkers", Department of Biochemistry and Biotechnology, University of Thessaly (to A-M.G.P. and S.I.M.).

Institutional Review Board Statement: Not applicable.

Informed Consent Statement: Not applicable.

Data Availability Statement: Data are contained within the article.

Acknowledgments: The authors would like to thank the "Chios Gum Mastic Growers Association" and the "mastihashop" for their kind donation of Chios Mastic Gum.

Conflicts of Interest: The authors declare no conflicts of interest.

Abbreviations

The following abbreviations are used in this manuscript:

CMG	Chios Mastic Gum
PCL	Poly-ε-caprolactone
SEM	Scanning electron microscopy
DSC	Differential scanning calorimetry
TGA	Thermogravimetric analysis
PDO	Protected designation of origin
GR	Glucocorticoid receptor
AMPK	AMP-activated protein kinase
PPARα	Peroxisome proliferator-activated receptor α
NF-κB	Nuclear factor-kappa B
PKC	Protein kinase C
oxLDL	Oxidized, low-density lipoprotein
NO	Nitric oxide
PEG2	Prostaglandin E2
EMA	European Medicines Agency
TMEWP	Total mastic extract without polymer
ECM	Extracellular matrix
UV	Ultraviolet
DCM	Dichloromethane
DMF	Dimethylformamide
DMEM	Dulbecco's modified Eagle medium
FBS	Fetal bovine serum
MTT	3-(4,5-dimethylthiazol-2-yl)-2,5-diphenyltetrazolium bromide
DMSO	Dimethyl sulfonyl chloride
ATCC	American Type Culture Collection

References

1. European Commission. Commission Regulation (EC) No 123/97 of 23 January 1997 Supplementing the Annex to Commission Regulation (EC) No 1107/96 on the Registration of Geographical Indications and Designations of Origin Under the Procedure Laid Down in Article 17 of Regulation (EEC) No 2081/92 (Text with EEA Relevance). 1997, pp. 19–25. Available online: https://eur-lex.europa.eu/legal-content/EN/TXT/PDF/?uri=CELEX:31997R0123 (accessed on 20 August 2025).
2. UNESCO. Decision of the Intergovernmental Committee: 9.COM 10.18. In *Inscription of "Traditional Know-How of Cultivating Mastic" on the Representative List of the Intangible Cultural Heritage of Humanity on the Island of Chios, Proceedings of the Intergovernmental Committee for the Safeguarding of the Intangible Cultural Heritage, Paris, France, 24–28 November 2014*; Ninth Session: Paris, France, 2014.
3. Georgantopoulos, A.; Kalousi, F.D.; Pollastro, F.; Tsialtas, I.; Kalogiouri, N.P.; Psarra, A.-M.G. Chemical Analysis and Antioxidant Activities of Resin Fractions from Pistacia lentiscus L. var. Chia in Neuroblastoma SH-SY5Y Cells. *Molecules* **2025**, *30*, 997. [CrossRef]
4. Pachi, V.K.; Mikropoulou, E.V.; Gkiouvetidis, P.; Siafakas, K.; Argyropoulou, A.; Angelis, A.; Mitakou, S.; Halabalaki, M. Traditional uses, phytochemistry and pharmacology of Chios mastic gum (Pistacia lentiscus var. Chia, Anacardiaceae): A review. *J. Ethnopharmacol.* **2020**, *254*, 112485. [CrossRef]
5. Marshall, B.J.; Warren, J.R. Unidentified curved bacilli in the stomach of patients with gastritis and peptic ulceration. *Lancet* **1984**, *1*, 1311–1315. [CrossRef] [PubMed]
6. Paraschos, S.; Magiatis, P.; Mitakou, S.; Petraki, K.; Kalliaropoulos, A.; Maragkoudakis, P.; Mentis, A.; Sgouras, D.; Skaltsounis, A.L. In vitro and in vivo activities of Chios mastic gum extracts and constituents against Helicobacter pylori. *Antimicrob. Agents Chemother.* **2007**, *51*, 551–559. [CrossRef]
7. Sharif Sharifi, M.; Hazell, S.L. Fractionation of Mastic Gum in Relation to Antimicrobial Activity. *Pharmaceuticals* **2009**, *2*, 2–10. [CrossRef]
8. Ottria, R.; Xynomilakis, O.; Casati, S.; Abbiati, E.; Maconi, G.; Ciuffreda, P. Chios Mastic Gum: Chemical Profile and Pharmacological Properties in Inflammatory Bowel Disease: From the Past to the Future. *Int. J. Mol. Sci.* **2023**, *24*, 12038. [CrossRef] [PubMed]
9. Dabos, K.J.; Sfika, E.; Vlatta, L.J.; Frantzi, D.; Amygdalos, G.I.; Giannikopoulos, G. Is Chios mastic gum effective in the treatment of functional dyspepsia? A prospective randomised double-blind placebo controlled trial. *J. Ethnopharmacol.* **2010**, *127*, 205–209. [CrossRef]
10. Koychev, S.; Dommisch, H.; Chen, H.; Pischon, N. Antimicrobial Effects of Mastic Extract Against Oral and Periodontal Pathogens. *J. Periodontol.* **2017**, *88*, 511–517. [CrossRef] [PubMed]
11. Faruque, M.R.J.; Potocka, W.; Nazmi, K.; Ligtenberg, A.J.; Bikker, F.J.; Laine, M.L. Scent of relief: Mastic resin scent recovers salivation in chronic dry mouth patients. *Biomed. Pharmacother.* **2024**, *178*, 117245. [CrossRef]
12. Duru, M.E.; Cakir, A.; Kordali, S.; Zengin, H.; Harmandar, M.; Izumi, S.; Hirata, T. Chemical composition and antifungal properties of essential oils of three Pistacia species. *Fitoterapia* **2003**, *74*, 170–176. [CrossRef]
13. Magiatis, P.; Melliou, E.; Skaltsounis, A.L.; Chinou, I.B.; Mitaku, S. Chemical composition and antimicrobial activity of the essential oils of Pistacia lentiscus var. chia. *Planta Med.* **1999**, *65*, 749–752. [CrossRef]
14. Gortzi, O.; Rovoli, M.; Katsoulis, K.; Graikou, K.; Karagkini, D.-A.; Stagos, D.; Kouretas, D.; Tsaknis, J.; Chinou, I. Study of Stability, Cytotoxic and Antimicrobial Activity of Chios Mastic Gum Fractions (Neutral, Acidic) after Encapsulation in Liposomes. *Foods* **2022**, *11*, 271. [CrossRef]
15. Kalousi, F.D.; Pollastro, F.; Karra, A.G.; Tsialtas, I.; Georgantopoulos, A.; Salamone, S.; Psarra, A.-M.G. Regulation of Energy Metabolism and Anti-Inflammatory Activities of Mastiha Fractions from Pistacia lentiscus L. var. chia. *Foods* **2023**, *12*, 1390. [CrossRef] [PubMed]
16. Cui, H.; Li, X.; An, X.-R.; Liu, W.; Yuan, T. Masticadienonic acid from Chios mastic gum mitigates colitis in mice via modulating inflammatory response, gut barrier integrity and microbiota. *Phytomedicine* **2023**, *108*, 154518. [CrossRef] [PubMed]
17. Triantafyllou, A.; Bikineyeva, A.; Dikalova, A.; Nazarewicz, R.; Lerakis, S.; Dikalov, S. Anti-inflammatory activity of Chios mastic gum is associated with inhibition of TNF-alpha induced oxidative stress. *Nutr. J.* **2011**, *10*, 64. [CrossRef]
18. Papada, E.; Forbes, A.; Amerikanou, C.; Torović, L.; Kalogeropoulos, N.; Tzavara, C.; Triantafillidis, J.K.; Kaliora, A.C. Antioxidative Efficacy of a Pistacia Lentiscus Supplement and Its Effect on the Plasma Amino Acid Profile in Inflammatory Bowel Disease: A Randomised, Double-Blind, Placebo-Controlled Trial. *Nutrients* **2018**, *10*, 1779. [CrossRef]
19. Andrikopoulos, N.K.; Kaliora, A.C.; Assimopoulou, A.N.; Papapeorgiou, V.P. Biological activity of some naturally occurring resins, gums and pigments against in vitro LDL oxidation. *Phytother. Res.* **2003**, *17*, 501–507. [CrossRef] [PubMed]
20. Zhou, L.; Satoh, K.; Takahashi, K.; Watanabe, S.; Nakamura, W.; Maki, J.; Hatano, H.; Takekawa, F.; Shimada, C.; Sakagami, H. Re-evaluation of anti-inflammatory activity of mastic using activated macrophages. *In Vivo* **2009**, *23*, 583–589.

21. Georgantopoulos, A.; Vougioukas, A.; Kalousi, F.D.; Tsialtas, I.; Psarra, A.-M.G. Comparative Studies on the Anti-Inflammatory and Apoptotic Activities of Four Greek Essential Oils: Involvement in the Regulation of NF-κB and Steroid Receptor Signaling. *Life* **2023**, *13*, 1534. [CrossRef]
22. Loutrari, H.; Magkouta, S.; Papapetropoulos, A.; Roussos, C. Mastic Oil Inhibits the Metastatic Phenotype of Mouse Lung Adenocarcinoma Cells. *Cancers* **2011**, *3*, 789–801. [CrossRef]
23. Kim, J.-H.; Choi, J.-H.; Jung, Y.-S.; Cho, M.-J.; Lee, Y.-E.; Park, D.-O.; Song, K.-B. Anticancer effect of mastic on human oral cancer cells. *J. Korean Acad. Oral Health* **2016**, *40*, 143–148. [CrossRef]
24. Balan, K.V.; Demetzos, C.; Prince, J.; Dimas, K.; Cladaras, M.; Han, Z.; Wyche, J.H.; Pantazis, P. Induction of Apoptosis in Human Colon Cancer HCT116 Cells Treated with an Extract of the Plant Product, Chios Mastic Gum. *In Vivo* **2005**, *19*, 93–102.
25. Sawidis, T.; Yurukova, L.; Askitis, T. Chios mastic, a natural supplement for zinc to enhance male sexuality and prostate function. *Pharm. Biol.* **2010**, *48*, 48–54. [CrossRef]
26. Triantafyllou, A.; Chaviaras, N.; Sergentanis, T.N.; Protopapa, E.; Tsaknis, J. Chios mastic gum modulates serum biochemical parameters in a human population. *J. Ethnopharmacol.* **2007**, *111*, 43–49. [CrossRef]
27. Kartalis, A.; Didagelos, M.; Georgiadis, I.; Benetos, G.; Smyrnioudis, N.; Marmaras, H.; Voutas, P.; Zotika, C.; Garoufalis, S.; Andrikopoulos, G. Effects of Chios mastic gum on cholesterol and glucose levels of healthy volunteers: A prospective, randomized, placebo-controlled, pilot study (CHIOS-MASTIHA). *Eur. J. Prev. Cardiol.* **2016**, *23*, 722–729. [CrossRef]
28. European Medicines Agency. *Assessment Report on Pistacia Lentiscus L., Resin (Mastix)*; Committee on Herbal Medicinal Products (HMPC): London, UK, 2016.
29. Bebb, J.R.; Bailey-Flitter, N.; Ala'Aldeen, D.; Atherton, J.C. Mastic gum has no effect on Helicobacter pylori load in vivo. *J. Antimicrob. Chemother.* **2003**, *52*, 522–523. [CrossRef]
30. Loughlin, M.F.; Ala'Aldeen, D.A.; Jenks, P.J. Monotherapy with mastic does not eradicate Helicobacter pylori infection from mice. *J. Antimicrob. Chemother.* **2003**, *51*, 367–371. [CrossRef]
31. Andreadou, I.; Mitakou, S.; Paraschos, S.; Efentakis, P.; Magiatis, P.; Kaklamanis, L.; Halabalaki, M.; Skaltsounis, L.; Iliodromitis, E.K. "Pistacia lentiscus L." reduces the infarct size in normal fed anesthetized rabbits and possess antiatheromatic and hypolipidemic activity in cholesterol fed rabbits. *Phytomedicine* **2016**, *23*, 1220–1226. [CrossRef]
32. El-Chaghaby, G.; Ahmad, A. Biosynthesis of silver nanoparticles using pistacia lentiscus leaves extract and investigation of their antimicrobial effect. *Orient. J. Chem.* **2011**, *27*, 929–936.
33. Zintle, M.; Siwaphiwe, P.; Marthe Carine, F.; Thierry Youmbi, F.; Derek Tantoh, N.; Suprakas Sinha, R.; Blessing Atim, A. Antibacterial study of carbopol-mastic gum/silver nanoparticle-based topical gels with carvacrol/neem bark extract in vitro. *J. Wound Care* **2023**, *32*, 182–189. [CrossRef] [PubMed]
34. Vrouvaki, I.; Koutra, E.; Kornaros, M.; Avgoustakis, K.; Lamari, F.N.; Hatziantoniou, S. Polymeric Nanoparticles of Pistacia lentiscus var. chia Essential Oil for Cutaneous Applications. *Pharmaceutics* **2020**, *12*, 353. [CrossRef]
35. Park, J.-H.; Yang, J.-Y.; Jeon, Y.; Kim, J.; Baek, J.-H. Evaluating the efficacy of curcumin and mastic gum enclosed in phospholipid-based lipid nanoparticles on Helicobacter pylori treatment using urea breath test delta values: A single-arm prospective pilot study. *Res. Sq.* **2024**. [CrossRef]
36. Selvaraj, K.; Lee, S.-J.; Song, K.-B.; Yoo, B.-K.; Karuppaiah, A. Fabrication of Mastic Gum Resin Tethered Phospholipid Nanocarriers for the Evaluation and Enhancement of Anti-inflammatory and Anti-bacterial Effects. *Curr. Pharm. Des.* **2025**, *31*, 1866–1876. [CrossRef]
37. Ao, F.; Yin, C.; Luo, X.; Shen, W.; Ge, X.; Zheng, Y. Controlled dual drug delivery system based on gelatin electrospinning membranes for wound healing promotion. *Int. J. Biol. Macromol.* **2025**, *289*, 138720. [CrossRef]
38. Eldem, A.; Tekintaş, Y.; Ucuncu, M.; Horzum, N. Electrospun Nanofiber Platforms for Photodynamic Therapy: Role and Efficacy in Cancer, Antimicrobial, and Wound Healing Applications. *Macromol. Mater. Eng.* **2025**, *310*, 2500014. [CrossRef]
39. Zheng, Z.; Zhang, H.; Yang, J.; Liu, X.; Chen, L.; Li, W.; Mi, S.; Zhou, H.; Zheng, W.; Xue, W.; et al. Recent advances in structural and functional design of electrospun nanofibers for wound healing. *J. Mater. Chem. B* **2025**, *13*, 5226–5263. [CrossRef]
40. Dong, Y.; Zheng, Y.; Zhang, K.; Yao, Y.; Wang, L.; Li, X.; Yu, J.; Ding, B. Electrospun Nanofibrous Materials for Wound Healing. *Adv. Fiber Mater.* **2020**, *2*, 212–227. [CrossRef]
41. Han, D.; Gouma, P.I. Electrospun bioscaffolds that mimic the topology of extracellular matrix. *Nanomedicine* **2006**, *2*, 37–41. [CrossRef]
42. Kayan, G.Ö.; Kayan, A. Polycaprolactone Composites/Blends and Their Applications Especially in Water Treatment. *ChemEngineering* **2023**, *7*, 104. [CrossRef]
43. Spartali, C.; Psarra, A.-M.G.; Marras, S.I.; Tsioptsias, C.; Georgantopoulos, A.; Kalousi, F.D.; Tsakalof, A.; Tsivintzelis, I. Silybin-Functionalized PCL Electrospun Fibrous Membranes for Potential Pharmaceutical and Biomedical Applications. *Polymers* **2024**, *16*, 2346. [CrossRef]

44. Marras, S.I.; Kladi, K.P.; Tsivintzelis, I.; Zuburtikudis, I.; Panayiotou, C. Biodegradable polymer nanocomposites: The role of nanoclays on the thermomechanical characteristics and the electrospun fibrous structure. *Acta Biomater.* **2008**, *4*, 756–765. [CrossRef]
45. Schneider, C.A.; Rasband, W.S.; Eliceiri, K.W. NIH Image to ImageJ: 25 years of image analysis. *Nat. Methods* **2012**, *9*, 671–675. [CrossRef]
46. Guo, Y.; Han, Z.; Zhang, J.; Lu, Y.; Li, C.; Liu, G. Development of a high-speed and ultrasensitive UV/Vis-CM for detecting total triterpenes in traditional Chinese medicine and its application. *Heliyon* **2024**, *10*, e32239. [CrossRef]
47. Yang, M.; Xiang, G.; Li, D.; Zhang, Y.; Xu, W.; Tao, L. The insecticide spinosad induces DNA damage and apoptosis in HEK293 and HepG2 cells. *Mutat. Res. Genet. Toxicol. Environ. Mutagen.* **2016**, *812*, 12–19. [CrossRef]
48. Kehinde, I.; Khan, R.; Nlooto, M.; Gordon, M. Modulatory influences of antiviral bioactive compounds on cell viability, mRNA and protein expression of cytochrome P450 3A4 and P-glycoprotein in HepG2 and HEK293 cells. *Bioorg. Chem.* **2021**, *107*, 104573. [CrossRef]
49. Al-Abduljabbar, A.; Farooq, I. Electrospun Polymer Nanofibers: Processing, Properties, and Applications. *Polymers* **2023**, *15*, 65. [CrossRef] [PubMed]
50. Shabani, A.; Al, G.A.; Berri, N.; Castro-Dominguez, B.; Leese, H.S.; Martinez-Hernandez, U. Electrospinning Technology, Machine Learning, and Control Approaches: A Review. *Adv. Eng. Mater.* **2025**, *27*, 2401353. [CrossRef]
51. Zhao, Y.-S.; Huang, J.; Yang, X.; Wang, W.; Yu, D.-G.; He, H.; Liu, P.; Du, K. Electrospun nanofibers and their application as sensors for healthcare. *Front. Bioeng. Biotechnol.* **2025**, *13*, 1533367. [CrossRef] [PubMed]
52. Pillay, V.; Dott, C.; Choonara, Y.E.; Tyagi, C.; Tomar, L.; Kumar, P.; du Toit, L.C.; Ndesendo, V.M.K. A Review of the Effect of Processing Variables on the Fabrication of Electrospun Nanofibers for Drug Delivery Applications. *J. Nanomater.* **2013**, *2013*, 789289. [CrossRef]
53. Yuan, Y.; Choi, K.; Choi, S.-O.; Kim, J. Early stage release control of an anticancer drug by drug-polymer miscibility in a hydrophobic fiber-based drug delivery system. *RSC Adv.* **2018**, *8*, 19791–19803. [CrossRef]
54. Goonoo, N.; Bhaw-Luximon, A.; Jhurry, D. Drug Loading and Release from Electrospun Biodegradable Nanofibers. *J. Biomed. Nanotechnol.* **2014**, *10*, 2173–2199. [CrossRef]
55. Luraghi, A.; Peri, F.; Moroni, L. Electrospinning for drug delivery applications: A review. *J. Control. Release* **2021**, *334*, 463–484. [CrossRef] [PubMed]
56. Eren Böncü, T.; Özdemir, N. Effects of drug concentration and PLGA addition on the properties of electrospun ampicillin trihydrate-loaded PLA nanofibers. *Beilstein J. Nanotechnol.* **2022**, *13*, 245–254. [CrossRef]
57. Blakney, A.K.; Krogstad, E.A.; Jiang, Y.H.; Woodrow, K.A. Delivery of multipurpose prevention drug combinations from electrospun nanofibers using composite microarchitectures. *Int. J. Nanomed.* **2014**, *9*, 2967–2978. [CrossRef] [PubMed]
58. Krogstad, E.A.; Woodrow, K.A. Manufacturing scale-up of electrospun poly(vinyl alcohol) fibers containing tenofovir for vaginal drug delivery. *Int. J. Pharm.* **2014**, *475*, 282–291. [CrossRef]
59. Aydogdu Emir, A.; Akgun, M.; Kirtil, E. Effect of mastic gum integration on improvement of polylactic acid biodegradable films. *Polym. Eng. Sci.* **2023**, *63*, 1539–1550. [CrossRef]
60. Kalousi, F.D.; Pollastro, F.; Christodoulou, E.C.; Karra, A.G.; Tsialtas, I.; Georgantopoulos, A.; Salamone, S.; Psarra, A.-M.G. Apoptotic, Anti-Inflammatory Activities and Interference with the Glucocorticoid Receptor Signaling of Fractions from Pistacia lentiscus L. var. chia Leaves. *Plants* **2022**, *11*, 934. [CrossRef]
61. Laskari, V.; Katsanou, E.; Kyriakopoulou, K.; Termentzi, A.; Skaltsounis, A.L.; Fokialakis, N.; Machera, K. In vitro protection and toxicity assessment of Chios Mastic Gum extracts and isolated triterpenic acids using human hepatocarcinoma cells. *Planta Med.* **2015**, *81*, PM_68. [CrossRef]
62. He, M.-L.; Yuan, H.-Q.; Jiang, A.-L.; Gong, A.Y.; Chen, W.-W.; Zhang, P.-J.; Young, C.Y.F.; Zhang, J.-Y. Gum mastic inhibits the expression and function of the androgen receptor in prostate cancer cells. *Cancer* **2006**, *106*, 2547–2555. [CrossRef]
63. He, M.-L.; Li, A.; Xu, C.-S.; Wang, S.-L.; Zhang, M.-J.; Gu, H.; Yang, Y.-Q.; Tao, H.-H. Mechanisms of antiprostate cancer by gum mastic: NF-κB signal as target. *Acta Pharmacol. Sin.* **2007**, *28*, 446–452. [CrossRef]
64. Koo, B.-C.; Kim, D.-H.; Kim, I.-R.; Kim, G.-C.; Kwak, H.-H.; Park, B.-S. A natural product, chios gum mastic, induces the death of HL-60 cells via apoptosis and cell cycle arrest. *Int. J. Oral Biol.* **2011**, *36*, 13–21.
65. Huang, X.-Y.; Wang, H.-C.; Yuan, Z.; Li, A.; He, M.-L.; Ai, K.-X.; Zheng, Q.; Qin, H.-L. Gemcitabine combined with gum mastic causes potent growth inhibition and apoptosis of pancreatic cancer cells. *Acta Pharmacol. Sin.* **2010**, *31*, 741–745. [CrossRef]
66. Li, S.; Cha, I.-H.; Nam, W. Chios mastic gum extracts as a potent antitumor agent that inhibits growth and induces apoptosis of oral cancer cells. *Asian Pac. J. Cancer Prev.* **2011**, *12*, 1877–1880.
67. Lee, S.-E.; Hur, Y.-J.; Kim, I.-R.; Kwak, H.-H.; Kim, G.-C.; Shin, S.-H.; Kim, C.-H.; Park, B.-S. Mechanism underlying Chios gum mastic-induced apoptosis on SCC25 human tongue squamous cell carcinoma cell line. *Int. J. Oral Biol.* **2009**, *34*, 61–72.

68. Espinoza, S.M.; Indrabhan, P.H.; Eduardo, S.M.M.; Rocio, C.P.; Ige, P.P. Poly-ε-caprolactone (PCL), a promising polymer for pharmaceutical and biomedical applications: Focus on nanomedicine in cancer. *Int. J. Polym. Mater. Polym. Biomater.* **2020**, *69*, 85–126. [CrossRef]
69. Mitxelena-Iribarren, O.; Riera-Pons, M.; Pereira, S.; Calero-Castro, F.J.; Castillo Tuñón, J.M.; Padillo-Ruiz, J.; Mujika, M.; Arana, S. Drug-loaded PCL electrospun nanofibers as anti-pancreatic cancer drug delivery systems. *Polym. Bull.* **2023**, *80*, 7763–7778. [CrossRef]
70. Rasekh, M.; Pisapia, F.; Nokhodchi, A. Innovative applications of electrospun nanofibers in cancer research. *J. Drug Deliv. Sci. Technol.* **2024**, *91*, 105255. [CrossRef]

Disclaimer/Publisher's Note: The statements, opinions and data contained in all publications are solely those of the individual author(s) and contributor(s) and not of MDPI and/or the editor(s). MDPI and/or the editor(s) disclaim responsibility for any injury to people or property resulting from any ideas, methods, instructions or products referred to in the content.